Experimental fire response of seismic elastomeric bearings

Massimiliano Lucon[1], Paolo Baragatti[1], Luca Possidente[2], Nicola Tondini[2]*

[1]INNOVA AE S.r.l. – Via di San Martino ai Monti 8, 00184, Roma, Italy
[2]University of Trento – Department of Civil, Environmental and Mechanical Engineering, Via Mesiano 77, 38123, Trento, Italy

*Corresponding author: nicola.tondini@unitn.it

Abstract

The paper presents the results of an experimental campaign conducted with the aim to evaluate the fire behaviour of unprotected and protected seismic elastomeric bearings installed inside an actual building. In particular, one unprotected and two protected natural rubber bearings were tested under the ISO 834 heating curve. The fire protection was made of blankets based on alkaline earth silicate wools (AES) of different thickness, i.e. 100 mm and 125 mm. The fire tests were performed by applying a constant vertical load equal to 900 kN to elastomeric bearings of diameter 400 mm, i.e. applied stress less than 10 MPa. The tests highlighted that the unprotected elastomeric bearing met the fire resistance requirement of 60 min before a loss of vertical load-bearing capacity owing to degradation of the mechanical properties at elevated temperature, whereas the protected elastomeric bearings could satisfy the fire resistance requirement of 90 min. A comprehensive description of the experimental outcomes, that also include the characterisation of the residual post-fire mechanical properties, is thoroughly reported in the paper.

Keywords

Seismic elastomeric bearings; rubber; fire; experimental tests; post-fire characterisation

1. Introduction

Seismic base-isolation represents an efficient way to protect a structure from strong earthquake events [1-4]. Seismic protection through base-isolation can be realised by means of different devices; to name a few: rubber bearings [1], sliding bearings [2,3], friction pendulums [4]. With respect to base-isolation made of rubber bearings, several works can be found in literature [1,5-8]. When base-isolation is employed, the superstructure is typically isolated at the ground level by interposing the bearings at the top of the columns of the first underground floor and the design is such to keep the structure elastic during the ground motion. At the same time, the underground floors are areas commonly dedicated to car parks whose fire risk is not negligible [9-13] and structural engineers must ensure an appropriate fire resistance of the structural system, that also includes the elastomeric bearings. Indeed, the seismic design can also affect the fire response of a structure [14]. Moreover, since base-isolation is often foreseen for buildings with large floor area and a fire may affect only a portion of it, the loss of vertical load-bearing capacity of rubber bearings due to material degradation at elevated temperature [15-17] may entail differential settlements that can undermine the structure functionality or even its stability. On these premises, it is paramount to provide the elastomeric bearings with sufficient fire resistance by also considering that they are located close to the ceiling level and consequently exposed to significant thermal action given the smoke accumulation [18,19]. The fire resistance of unprotected rubber bearings in the first stages is influenced by the low value of thermal conductivity of the rubber that prevents a fast temperature increase within the isolator, but when the vulcanization temperature between layers of rubber and steel plates is exceeded, quick degradation of the mechanical properties occurs [15,20]. Effect of heating on the behaviour of Lead-Rubber Bearings (LRBs) subjected to cyclic loading was studied [21-23] and heat transfer analyses were performed, but they did not specifically deal with the effect of fire. Mazza [24] applied incremental dynamic analysis to fire-damaged reinforced concrete structures with fire-protected High-Damping-Laminated-Rubber Bearings (HDLRBs). Thus, despite the structural fire behaviour was considered, no degradation was applied to the rubber bearings because of the fire protection. On

these premises, there is a paucity of studies about the fire behaviour of elastomeric bearings. In greater detail, at numerical level, a few works by the same main author that include the fire behaviour of rubber bearings can be found [25-28] and they mainly deal with the residual seismic capacity of fire-damaged elastomeric bearings. In greater detail, in [25] the analysis of the fire behaviour of unprotected HDLRBs and LRBs was included by means of 3D heat transfer analysis considering parametric fire curves applied to the vertical sides of the bearings. It was then proposed the 200 °C isotherm method that specifies a threshold temperature equal to 200°C for the residual cross-section of HDLRBs and of LRBs that neglects rubber with temperatures exceeding the vulcanization threshold with steel shims and keeps unaffected the mechanical properties of the remaining part of the bearing, which means that in the analysis the rubber bearing is considered with a reduced radius. In [26] the torsional response of fire-damaged base-isolated buildings with elastomeric bearings subjected to near-fault earthquakes was analysed. Based on the outcomes of [25], the 200°C isotherm method was applied in order to take into account the behaviour of fire-damaged HDLRBs. In [27] similar analyses were performed by investigating the aftershock behaviour of reinforced concrete base-isolated framed structure with fire-induced damage. The 200°C isotherm method was again applied to the rubber bearings to allow for the fire damage. In [28] fragility curves were derived on reinforced concrete seismically-isolated structures with residual mechanical properties after fire exposure. In order to allow for the mechanical degradation at elevated temperature the 150°C isotherm method was applied, which relies on the same concept of the 200°C isotherm method but with reduced threshold temperature to 150°C. It is worth noting that the proposed isotherm method is based on the vulcanization threshold temperature and, despite it is a good measure, it was not comprehensively validated against experimental data because of the lack of it. Moreover, since only reinforced concrete structures were investigated, the effect of the top and of the bottom boundary conditions on the thermal field in the bearing were not thoroughly analysed because concrete is characterised by low thermal conductivity and heat transfer in the vertical direction is less significant than in the radial direction. Indeed, at experimental level only a few studies can be found in literature

[29-31]. In this respect, Wu et al. [29] tested four unprotected and one protected lead rubber bearings and two unprotected and one protected natural rubber bearings subjected to the ISO 834 heating curve. All of them were characterised by diameter equal to 620 mm. They found that the influence of the vertical load is low on the residual mechanical properties and on the fire resistance. Moreover, they observed that tested unprotected rubber bearings could not resist a standard fire exposure of more than 90 min. Finally, they proposed a cementitious fire-insulation that met the fire resistance requirement of 180 min. More recently, Lan et al. [30] tested unprotected rubber bearings of diameter 520 mm that lasted 82 min exposed and designed a fire protection system. In [31] the fire response of the fire protected seismic rubber bearings with a large diameter of 1500 mm in the new airport of Beijing was analysed by means of fire tests and numerical modelling.

It is clear that more data and experimental evidence are needed to better understand the fire behaviour of elastomeric bearings. For instance, the temperature at which the mechanical properties of the rubber bearing start to markedly decrease was assumed by Mazza [25-27] as 200°C for HDLRBs and LRBs. In a subsequent work, the same author [28] proposed the same method with a reduced temperature, i.e. 150°C. Lan et al. [30] also proposed 150°C based on experimental evidence. Moreover, based on the results on unprotected rubber bearings, Wu et al. [29] designed the fire protection to prevent temperatures in the rubber higher than 107°C. Thus, this work aims at providing further experimental outcomes on the fire characterisation of unprotected and protected elastomeric bearings in the context of an actual design project. Indeed, the new experimental data will benefit practitioners and researchers for a better understanding of the fire behaviour of such devices and as a benchmark to calibrate analytical/numerical models that can allow for the degradation of rubber bearings owing to elevated temperature.

2. Description of the Case Study

The seismic devices studied in this work are part of an actual design project being underway in Rome. The case study consists of an urban area on which 5 different buildings with a unique sliding plane

and an underground car park are being built. The buildings are 5 storeys high or less and have different occupancy, i.e. an office building, a conference hall, a company canteen, a wellness centre and a warehouse space. Except for the conference hall, the buildings are connected at the level of the 4th and 5th floor. The car park covers more than 3000 square meters and has an inter-storey height of 2.9 meters. Seismic isolators are installed at the top of the concrete-filled columns of the car park to mitigate the effects of seismic actions, as shown in Figure 1.

a) b)

Figure 1. Isolators installed at the top of the columns located at the 1st underground floor.

In detail, 212 seismic elastomeric bearings are adopted. The main features of the 5 different type of seismic bearings employed are summarised in Table 1. The name of each device contains information about: the type of rubber (S, N, and H for Soft, Normal and Hard rubbers); the diameter of the isolator and the thickness of the rubber layers. For instance, the SI-S 400/100 bearing consists of a Seismic Isolator with Soft rubber with an overall diameter of 400 mm and with a total thickness of the rubber layers of 100 mm. In addition, Table 1 provides for each device, the total height, its section factor and the quantities installed, as well as the percentage over the total number of devices. Indeed, despite the section factor is usually employed for steel elements, it can be assumed that it still provides a good measure to indicate the sensitivity of the elastomeric bearings to heating by relating the exposed surface (A) to the volume (V) of the element. In this respect, the section factor was only used for selection purposes.

Table 1. Installed seismic bearings

Seismic device	Diameter [m]	Height [m]	A/V [m^{-1}]	Number of installed devices	
SI-S 400/100	0.40	0.178	10.0	62	29.2%
SI-S 450/102	0.45	0.190	8.9	25	11.8%
SI-S 500/102	0.50	0.190	8.0	36	17.0%
SI-S 600/104	0.60	0.180	6.7	45	19.8%
SI-S 700/100	0.70	0.177	5.7	26	12.3%
SI-S 800/100	0.80	0.177	5.0	21	9.9%
			TOT.	212	100%

According to the Ministerial Decree dated 1st February 1986 [32], vertical elements in the car park must maintain their load-bearing capacity for 90 minutes (R90) under the ISO 834 heating curve to meet the fire resistance requirements in accordance with a prescriptive approach. In order to understand whether the isolators can provide sufficient bearing capacity after 90 minutes, the most critical bearings were selected for experimental testing. Among the others, the SI-S 400/100 isolator presents the highest section factor. Moreover, the ratio between the demand and the capacity of the elastomeric rubber bearings (*D/C*) was calculated. The demand *D* for each of the 212 devices was determined according to the load combination in the fire situation in accordance with the Italian Building Code [33]

$$G_{1k} + G_{2k} + \psi_{21} Q_{1k} + \psi_{22} Q_{2k} + \cdots \quad (1)$$

Where G_{1k} and G_{2k} are the characteristic permanent loads, differentiated according to the self-weight of the structural members and the weight of the non-structural elements, respectively, while Q_{ik} and ψ_{2i} are the variable actions and the combination factor for the quasi-permanent value of the variable action in fire situation. It was found that the bearings from the first five series in Table 1 (with an overall diameter between 400 mm and 700mm) had a Demand (*D*) over Capacity (*C*) ratio in the range $0.5 \leq D/C \leq 0.6$, whereas for the SI-S 800/100 bearing, the ratio *D/C* was always lower than 0.3. As a consequence, the SI-S 400/100 isolator was selected since it exhibited the highest utilisation ratio (*D/C*) in the fire condition and it was characterised by the highest section factor.

3. Description of the experimental campaign

The experimental campaign was carried out on three specimens to evaluate the performance in the fire situation of the SI-S 400/100 bearing with and without fire protection. The geometrical and mechanical properties of the bearing are summarised in Table 2.

Table 2. Geometrical and mechanical properties of the SI-S 400/100 bearing according to European standard EN 15129:2009 [35].

SI-S 400/100 - Geometrical properties		
Overall diameter	D	400 mm
Effective diameter	D’	380 mm
Thickness of an individual elastomer layer	t_r	5 mm
Number of elastomer layers	n	20
Thickness of steel reinforcing plates	t_s	2 mm
Thickness of outer steel reinforcing plates (upper/lower)	t_{so}	20 mm
Thickness of steel anchor plates (upper/lower)	t_{sanch}	25 mm
Isolator height excluding steel anchor plates	h	178 mm
Isolator height including steel anchor plates	H	228 mm
Side length of steel anchor plates	Z	450 mm
SI-S 400/100 - Mechanical properties		
Dynamic shear modulus of the elastomer	G_{dyn}	0.40 MPa
Bulk modulus of the elastomer	E_b	2000 MPa
Yield stress of steel reinforcing plates	f_y	275 MPa

The test setup is depicted in Figure 2.

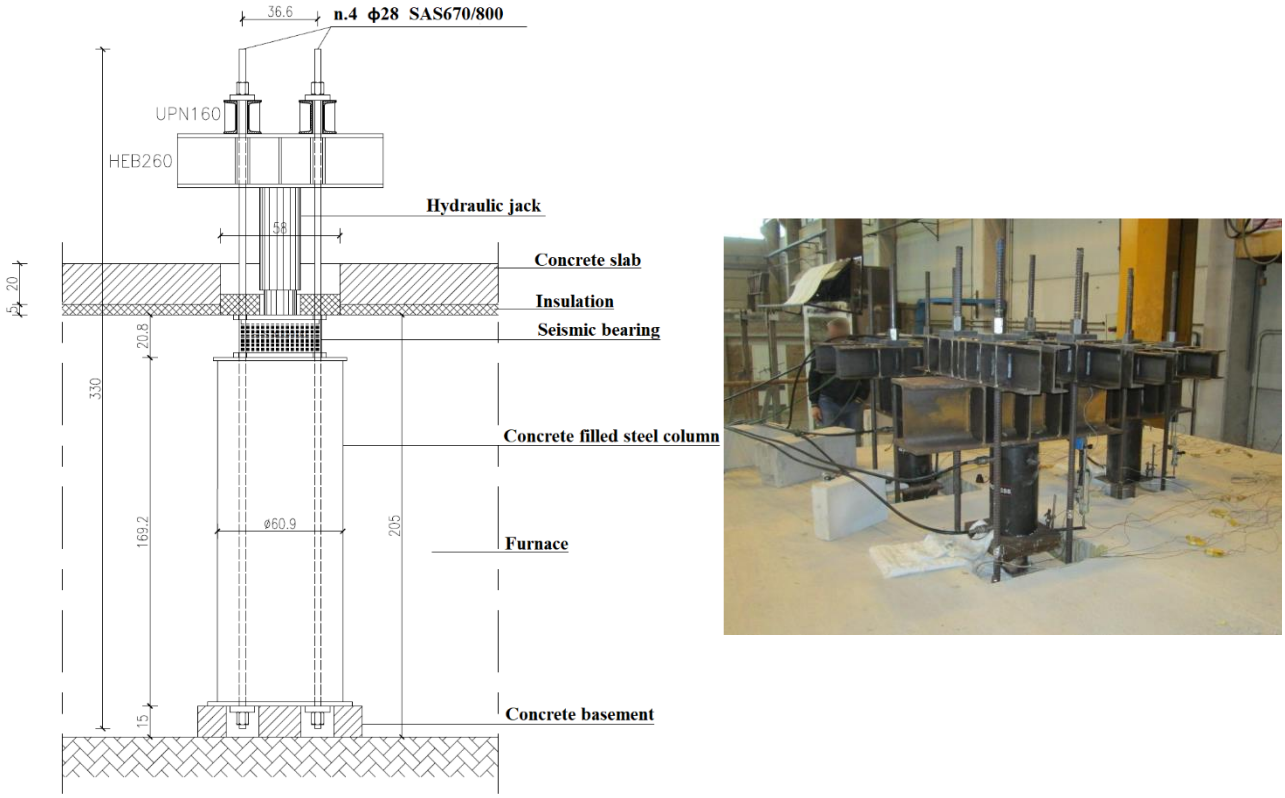

Figure 2. Test setup. Dimensions in cm.

Figure 3. Installation of the isolators on the top of the composite columns.

Each specimen was made of a circular concrete-filled steel column 1692 mm high, with diameter equal to 609 mm and the isolators mounted on the top. The specimens were installed inside a furnace and the height of the column was such that the top surface of the bearings and the inner surface of the furnace were aligned. Four steel bars SAS 670/800, with diameter of 28 mm and a length of 3300 mm, were embedded in the columns. These bars, together with steel plates at the ends of the columns,

allowed for fixing the specimens to a concrete basement 150-mm thick at the bottom of the furnace and to the load redistribution beam outside of the furnace, as shown in Figure 2. Indeed, the column-isolator systems were realised by simply placing the isolators on the top of the columns and letting the SAS 670/800 steel bars pass through four holes drilled in the corners of the top and the bottom plates of the isolators, as illustrated in Figure 3. The loading system consisted of UPN 160 and HE 260 B beams and a hydraulic jack. A load of 900 kN was applied, which was the highest load acting on the SI-S 400/100 bearings in the fire situation, i.e. 60% of the maximum vertical design load of the bearings. The load was controlled and applied directly on the upper plate of the isolators, on which the applied stress was less than 10 MPa. A pressure gauge allowed for measuring and control the load intensity to keep it constant during the test.

During the test, the temperature inside the furnace was imposed according to the ISO834 fire curve. The temperatures of the ISO834 curve, together with the temperatures recorded inside the furnace as a function of time are depicted in Figure 4a. Nine burners were employed to increase the temperature. The inner walls of the furnace were made of fire-resistant bricks, while a concrete slab 200-mm thick, with three holes for the specimens, was placed to close the furnace on the top. The bottom face of the concrete slab was covered with a thermal insulation of 12 mm. Fire protection was also placed on the top of the isolator to prevent the hot gases to flow outside the furnace.

In the first test, namely Test A, the isolator was not fire-protected, while in Tests B and C the isolators were covered with 4 and 5 layers of insulation blankets, respectively (Figure 4b). The thermal properties of rubber at ambient temperature are given in Table 3. It is evident that it has a much lower value of thermal diffusivity, defined as $\alpha = \lambda / \rho\, c_p = 1.012 \cdot 10^{-7}$ m^2/s, than steel, i.e. $\alpha = 1.15 \cdot 10^{-3}$ m^2/s. This entails lower rate of transfer of heat from hotter to colder parts. The fire protection was made of 25-mm thick blanket based on alkaline earth silicate wools (AES). Hence, the total thickness of the insulation wrapped around the isolators was of 100 mm and 125 mm for the Isolator B and C, respectively. The insulation properties of the fire protection are reported in Table 4. In all the specimens, the SAS 670/800 steel bars were insulated with 2 layers of the same insulation blanket.

Temperatures were recorded at five points along the vertical axis of the bearings and at two diametrical points at half of the height of the bearing, as illustrated in Figure 4c. In order to preserve the loading equipment and to continue the test successfully, thermocouples were also applied on the loading systems, in particular on the hydraulic jacks to keep the temperature under control. In Test A, three SAS 670/800 bars were also instrumented with thermocouples. The deformation of the seismic isolators during the tests was measured with displacement transducers.

Table 3. Thermal properties of rubber and steel at ambient temperature.

	Density ρ (kg/m^3)	Thermal conductivity λ (W/mK)	Specific heat c_p (J/kgK)
Rubber	1200	0.17	1400
Steel shims and plates	7850	50	450

Table 4. Thermal properties of the fire protection.

Density ρ (kg/m^3)	128 (at 20°C)
Specific heat c_p (J/kgK)	1130 (at (20°C)
Thermal conductivity λ (W/mK)	
200°C	0.06
400°c	0.10
600°c	0.16
800°C	0.23
1000°C	0.32

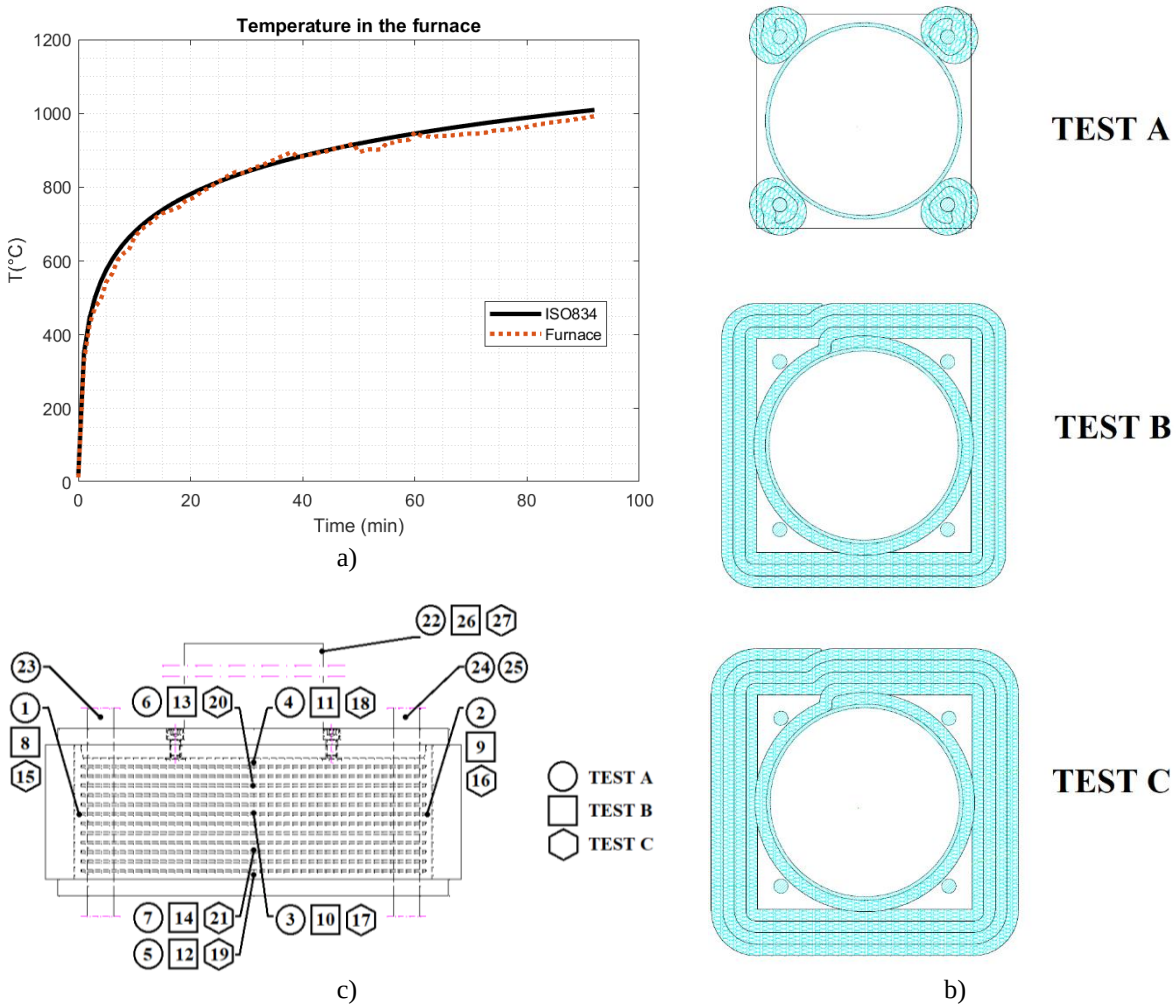

Figure 4. a) Temperature inside the furnace; b) Thermal insulation of the isolators; c) Thermocouples position.

3.1. Fire performance

Before the fire test, the specimens were stored in the laboratory for three days so as to reach thermal equilibrium with the ambient. Hence, the initial temperature of the specimens equalled the ambient temperature in the laboratory, i.e. $T_{in}=T_{am}=13°C$. Initially, the vertical load was applied to each isolator and it was kept constant for 15 min before starting the burners and applying the ISO 834 heating curve. The total duration of the fire test was equal to 92 minutes. After 20 minutes from the start of the fire test, water vapour and some smoke began to outflow from the hole in the slab above the unprotected isolator, i.e. Isolator A, which lost its vertical load-bearing capacity after 61 min. Conversely, the fire protected isolators, i.e. Isolator B and C, maintained their load-bearing capacity

for 92 min, time at which the furnace was stopped because flames came out from the hole of Isolator A that made the continuation of the test difficult. Thus, even if the performance could be higher, the fire resistance requirement of 90 min was met for both Isolator B and C. Figure 5 shows the conditions of the isolators after the fire test. It is possible to observe in Figure 5a and b that Isolator A underwent significant damage and loss of stability with the steel shim plates clearly visible and the rubber highly degraded falling apart. The bars used to apply the load were also damaged and bent with one that even broke. Conversely, in Figure 5c and d Isolators B and C are not visibly damaged with the rubber still in place. However, they were not totally unaffected by the fire as reported in Section 3.2, where the post-fire characterisation of both fire-protected isolators, i.e. Isolator B and C, is reported. Indeed, high temperatures were reached in the proximity of the plates during the fire test. These regions were affected by deterioration of the rubber that caused the bottom plates to detach.

a)

b)

c) d)

Figure 5. Conditions of the isolators after the fire test: a) Isolator A; b) Isolator B; c) Isolator C.

During the test, the increase of temperature $T-T_{in}$ was recorded by the thermocouples and the collected measurements are shown in Figure 6. For sake of brevity, from now on the increase of temperature measured by the thermocouples is simply referred as temperature, though the values in Figure 6 represent the $T-T_{in}$ quantity.

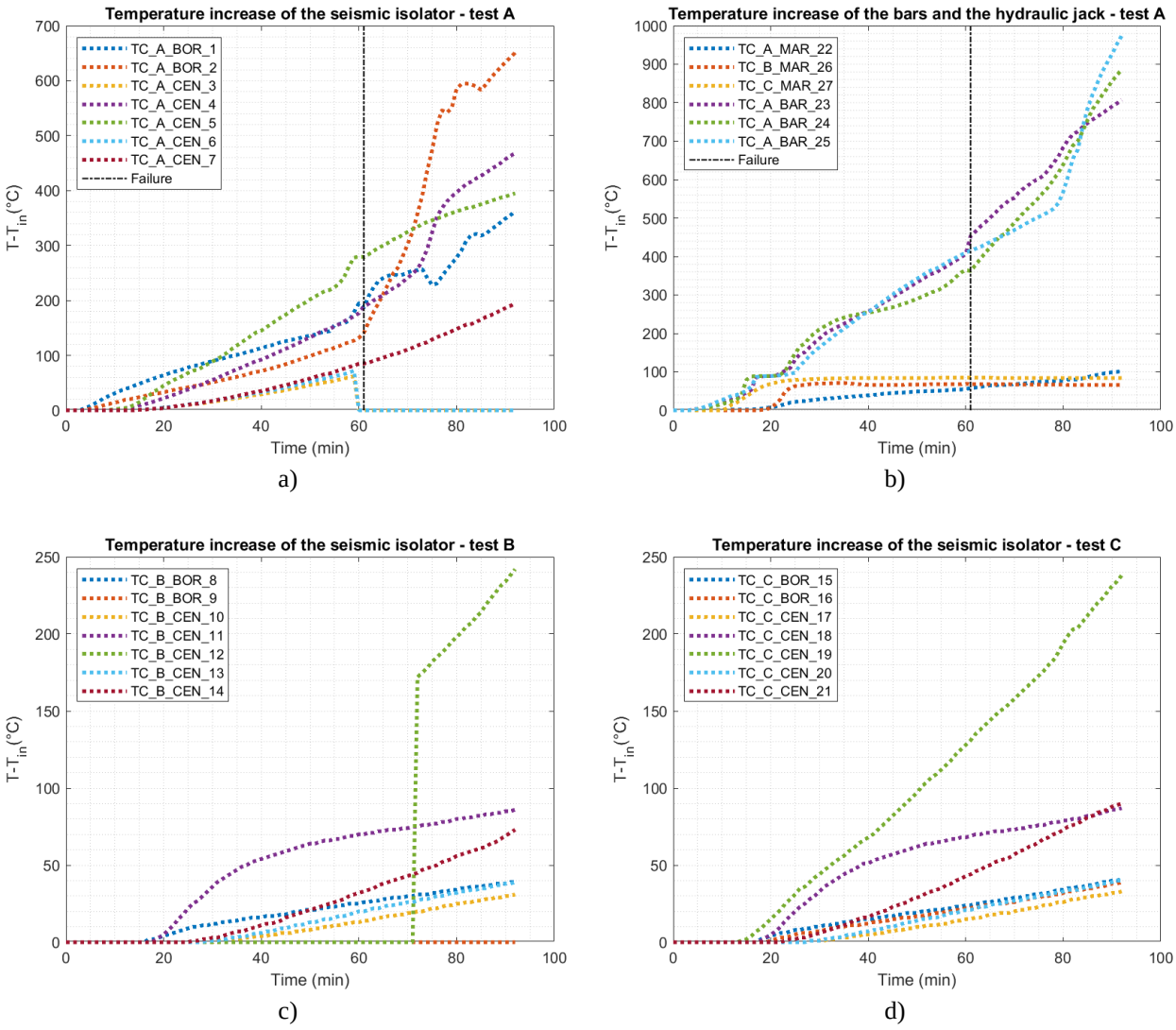

Figure 6. Temperatures recorded by the thermocouples: a) Isolator A; b) bars and plates of Isolator A; c) Isolator B; d) Isolator C.

Technical issues were encountered with Thermocouples 3 and 6 in Test A and Thermocouples 9 and 12 in Test B. In detail, Thermocouples 3 and 6 stopped working after 59 minutes, and 62°C and 72°C were the last recorded temperatures (Figure 6a). Thermocouple 12, instead, provided information only after 71 minutes (see Figure 6c) but by looking at the data in Figure 6d recorded by Thermocouple 19 installed in the same position on Isolator C, the reading seems to be reliable from time 71 min on because the temperature values are comparable. Thermocouple 9 never worked during the whole test. Nevertheless, though incomplete, the information provided by Thermocouples 3, 6 and 12 are reported.

It is interesting to note that in Tests B and C the highest temperatures were registered by Thermocouples 11, 12 and 18, 19 which were the closest to the steel plates of the isolators. It is reasonable to assume that higher temperatures are found at the top and bottom plates compared to the ones inside the isolators due to the heat sink effect of the steel plates. Similar behaviour was observed in Test A, during which Thermocouple 5 exhibited higher temperature increase during the fire evolution up to the isolator failure. Indeed, the temperature recordings after loss of load-bearing capacity are not reliable because the bearing was significantly damaged and its lateral rubber surface was charred and falling apart, exposing some thermocouples to different boundary conditions. Looking at the data recorded by the thermocouples installed inside the isolators along their vertical axis, i.e. Thermocouples 3, 6, 7 for Test A, Thermocouples 10, 13, 14 for Test B and Thermocouples 17, 20, 21 for Test C, it is possible to observe that for both unprotected and protected solutions the temperature remained below 100°C during the whole duration of the tests up to failure or the end of the test. This means 61 min for Isolator A and 92 min for Isolators B and C, respectively.

Figure 6b shows the temperatures of the hydraulic jacks, as well as the temperatures of three of the steel bars of test A. The loading equipment was well isolated since temperatures never exceeded 100°C and thus, the correct functioning of the hydraulic jacks was not jeopardised. Instead, higher temperatures were registered for the SAS 670/800 steel bars. Indeed, at about 20 minutes the thermocouples were possibly partially exposed to the hot gases because a sudden increase of temperature was recorded, as illustrated in Figure 6b. Nevertheless, the temperature of the rebars at the isolator failure, i.e. about 400°C, was not high enough to affect the mode of collapse. In fact, 400°C in a quenched and tempered steel bar means a yield strength reduction of about 0.7 with respect to the ambient temperature value [34], whereas the collapse would have occurred with degradation of the yield strength of about 0.55. It is worth mentioning that despite the loss of stiffness of the steel rebars owing to the temperature, since the load was controlled, it did not affect the applied load and consequently the mode of collapse. The temperature recordings after failure of the isolator are thus not relevant because the thermocouples were completely exposed to the hot gases, as compared in

Figure 4a and Figure 6d. In fact, at 92 minutes the temperatures of Thermocouples 23-25 were significantly high and the measurement of Thermocouple 22 was about the same as the one within the furnace. All the temperatures recorded after 61 and 92 minutes are reported in Table 5.

Table 5. Temperature increments of the seismic devices.

				Temperature increase $\Delta T=T-T_{in}$ at	
Test	Position of the thermocouple	Number	Label	61 min [°C]	92 min [°C]
A	Vertical border	1	TC_A_BOR_1	187	362
A	Vertical border	2	TC_A_BOR_2	141	651
A	Central vertical axis	3	TC_A_CEN_3	62*	//
A	Central vertical axis	4	TC_A_CEN_4	189	468
A	Central vertical axis	5	TC_A_CEN_5	279	395
A	Central vertical axis	6	TC_A_CEN_6	72*	//
A	Central vertical axis	7	TC_A_CEN_7	85	195
B	Vertical border	8	TC_B_BOR_8	26	39
B	Vertical border	9	TC_B_BOR_9	//	//
B	Central vertical axis	10	TC_B_CEN_10	14	31
B	Central vertical axis	11	TC_B_CEN_11	70	86
B	Central vertical axis	12	TC_B_CEN_12	//	242
B	Central vertical axis	13	TC_B_CEN_13	20	39
B	Central vertical axis	14	TC_B_CEN_14	33	73
C	Vertical border	15	TC_C_BOR_15	24	41
C	Vertical border	16	TC_C_BOR_16	22	39
C	Central vertical axis	17	TC_C_CEN_17	15	33
C	Central vertical axis	18	TC_C_CEN_18	69	87
C	Central vertical axis	19	TC_C_CEN_19	131	238
C	Central vertical axis	20	TC_C_CEN_20	21	40
C	Central vertical axis	21	TC_C_CEN_21	44	90

* Last recorded temperature increase at 59 min.

The axial displacement of the columns with the isolators on top was measured with respect to a fix point during the entire fire test for Isolators B and C and up to failure for Isolator A. This measure was mainly, at least in the first parts of the test, affected by the axial dilatation of the steel tube composing the composite column. As shown in Figure 7b, both the fire protected and unprotected seismic bearings experienced a similar displacement history. Due to the vertical load application at ambient temperature, shortening was recorded at first, with some difference among the isolators owing to the inherent variability of the properties of the loading system, of the rubber bearings and of the concrete-filled columns. Then, with the increase of the temperature, the columns gradually

expanded up to a peak deformation, that occurred in the 20-26 minute range. Then, a decrease in displacement was observed because of the loss of strength and stiffness of the steel tube and the load was mainly transferred to the concrete core with no significant variation in displacement until towards failure of Isolator A and the end of the test for Isolator B and C. Finally, a clear displacement decrease was detected. In greater detail, for Test A the decrease in displacement was associated with loss of stability and load-bearing capacity of the rubber isolator, whereas for Tests B and C, it hints the beginning of the loss of some mechanical properties and in particular of the vertical stiffness of the isolators close to the bottom plate. It is worth noting that a marked decrease of axial displacement started after 45 min for Isolator A and after 75 min for Isolator B and C, respectively. At these times, the temperature at the top and at the bottom of the rubber bearings was: 121°C (Thermocouple 4) and 182°C (Thermocouple 5) for Isolator A; 89°C (Thermocouple 11) and 191°C (Thermocouple 12) for Isolator B; 88°C (Thermocouple 18) and 183°C (Thermocouple 19) for Isolator C. This indicates that the boundary conditions at the top and bottom were essentially the same independently from the fire protection. Given the contact of the steel plates, it is reasonable to assume that the entire top and bottom surfaces were characterised by such values of temperature (or higher when approaching the borders). Based on these observations it may be stated that when the rubber temperature exceeds a temperature of 180°C, the loss of rubber mechanical properties starts significantly affecting the axial response of the bearing. This finding lies in between the threshold value (+20%) assumed in [28] and proposed in [30], i.e. 150°C, and the threshold value (-10%) assumed in [25-27] for the isotherm method, i.e. 200°C. It is clear that the loss of load-bearing capacity of Isolator A was primarily affected by the temperature increase in the radial direction because of the lack of protection. It is interesting to note that Test C experienced higher dilatation because, as depicted in Figure 7a, its position in the furnace was less shielded by the other specimens. Thus, the steel tube was hotter with respect to the other two specimens that underwent more comparable axial displacement because of symmetrical position. This is also confirmed by an early decrease in axial displacement for Test C at 20 min due to the loss of strength and stiffness of the steel tube.

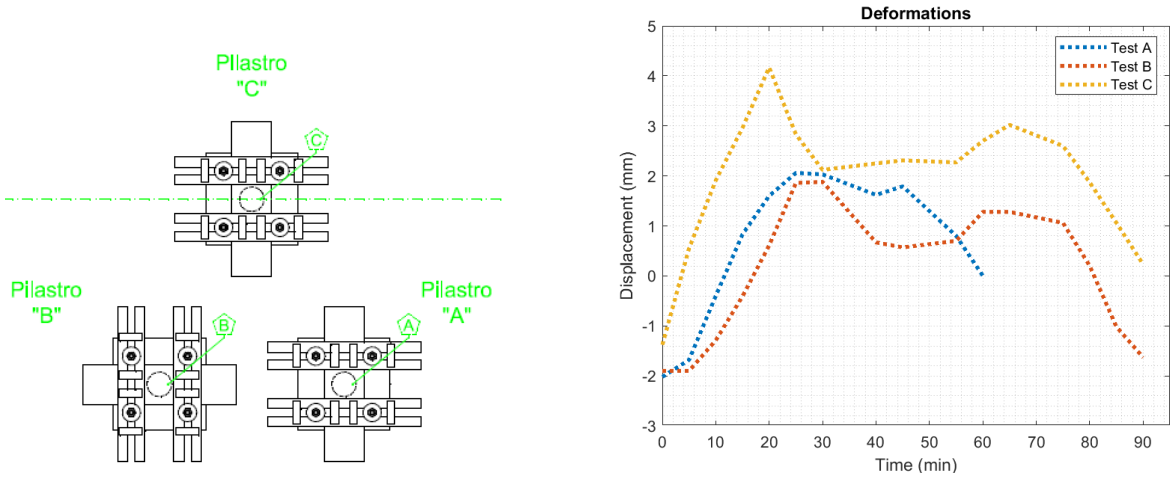

Figure 7. a) Position of the specimens in the furnace; b) axial displacements of the specimens during the fire test.

3.2. Pre- and post-fire mechanical characterisation

In this section the comparison between the axial mechanical properties pre- and post-fire of the isolators is reported. Indeed, mechanical characterisation at ambient temperature on similar bearings and after the fire test on Isolator B and C was performed by means of compression tests. The compression tests were performed according to EN 1337-3 [35]. The first step of the compression tests consisted in the application for one minute of the maximum load, which was equal to 929 kN for Isolator B and 931 kN for Isolator C, respectively. Then, after one minute the load was released and after further 10 minutes a compressive load with rate equal to 5 MPa/min was applied and the axial displacements were measured. The maximum load was kept constant for one minute, during which a visual inspection of the specimens was performed. A similar procedure was used for the post-fire characterisation of Isolator B and C, but these were tested without the bottom plates. Indeed, even though these isolators were protected, high temperatures were reached in the proximity of the plates during the fire test. These regions were affected by deterioration of the rubber that caused the bottom plates to detach. The load-displacement curves of the tested isolators are shown in Figure 8.

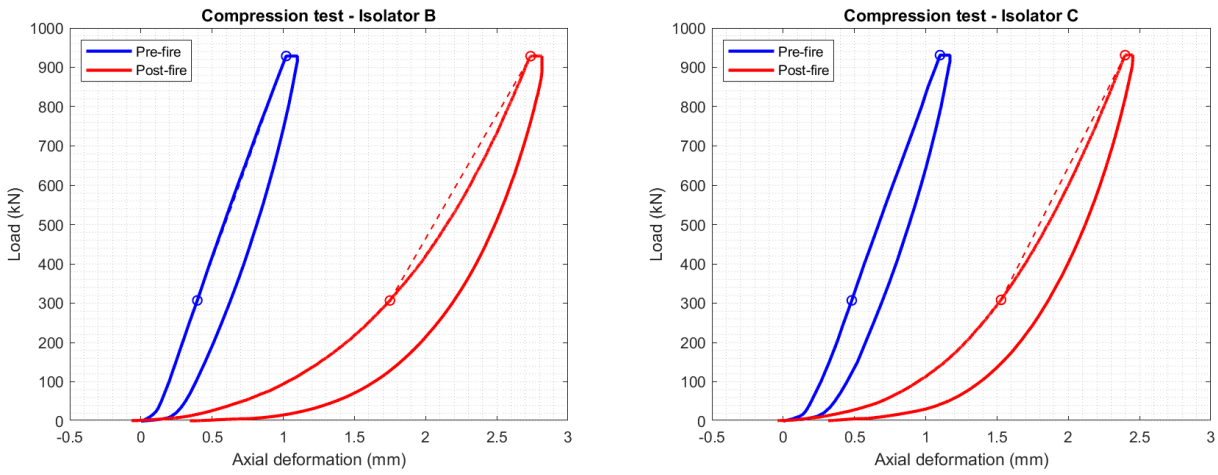

Figure 8. Characterisation before and after fire – Axial load vs. axial displacement

It is evident that the seismic bearings suffered of a significant loss of vertical stiffness due to the thermal attack, whereas the load-bearing capacity was essentially unaffected. In addition, while at ambient temperature a linear force-displacement behaviour was obtained after few loading steps, in the post-fire characterisation the axial stiffness of the isolators had a marked non-linear behaviour. Hence, the secant vertical stiffness K_v before and after fire is compared in Table 6. K_v was evaluated between two points, at 30% and 100% of the applied load. Both the isolators showed a comparable loss of stiffness, being 37.5% and 29.2% the total amount of the reduction of the secant vertical stiffness for the device B and C, respectively. It is worth noting that the lateral mechanical properties could have also been somehow affected owing to fire exposure. However, having a limited number of samples, it was decided not to investigate them, because in case of fire gravitational loads are predominant and the characterisation of the vertical axial behaviour is more relevant. Moreover, the replacement of the protected bearings is foreseen after the fire event.

Table 6. Post-fire characterisation.

Test		Axial load [kN]	Axial deformation [mm]		Vertical stiffness K_v [kN/mm]	
			Before the fire test	After the fire test	Before the fire test	After the fire test
B	0.30% N_{max}	307	0.40	1.75	1001	626
	100% N_{max}	929	1.02	2.74		
C	0.30% N_{max}	308	0.48	1.53	1004	711

100% N_{max}	931	1.10	2.40

After the post-fire characterisation, the devices were cut longitudinally for visual examination. Figure 9 shows the lateral rubber surface and the inner longitudinal section of the devices B (see Figure 9a and b) and C (see Figure 9c and d). Only the first layer of rubber, which was in contact with the bottom plate, reached very high temperatures during the fire test and it was severely deteriorated. The other rubber layers, as well as the rubber on the external surface, were in good conditions.

a) b)

c) d)

Figure 9. Visual inspection of Isolators B and C after the fire test.

3.3. Discussion of the results

The main results of the fire test are summarised in Table 7. The seismic bearing without fire protection, i.e. Isolator A, did not meet the R90 requirement and failure occurred at 61 minutes, while

both Isolators B and C, protected with 4 and 5 layers of insulation respectively, withstood the applied load until the end of the fire test at 92 min. Failure of Test A can be associated with the temperatures measured inside the seismic device. In this respect, vulcanized natural rubber begins to decompose and suffers of a rapid deterioration with an almost complete loss of strength when the threshold temperature of vulcanization is exceeded. As described in the introduction, Mazza [25-27] assumed 200°C to apply the so-called 200°C isotherm method, whereas in a later study, Mazza and Alesina [28] used a more conservative value of 150°C to apply the isotherm method. Based on experimental data, Lan et al. [30] observed, that 150°C was a representative threshold temperature value. In this work, a threshold value of about 180°C was found. Indeed, when the bottom layers of the rubber in contact with the steel plate exceeded 180°C, for each test a marked decrease in mechanical properties was observed with a steep drop in axial displacement. This hints that a value equal to 150°C represents a reasonable design threshold temperature. In addition, the influence of the boundary conditions applied to the steel plates should be carefully considered. Indeed, if not adequate detailing is applied, the contact of the plates with unprotected steel parts can cause significant heat transfer in the vertical direction and rubber degradation occurs both in radially and vertically. In this case, 3D heat transfer analysis is recommended. Moreover, Wu et al. [29] designed the fire protection to prevent temperatures in the rubber higher than 107°C. Thus, considering that thermocouples measured the increase of temperature with respect to the initial temperature T_{in}=13°C, the temperatures of all the external measure points exceeded the vulcanization threshold at 61 minutes in Test A, as shown in Figure 6. Indeed, though at failure the temperature of the inner points did not exceed 100°C, the more external thermocouples recorded much higher temperatures. In particular, the readings from the thermocouples on the bottom and top rubber layers (Points 5 and 4 in Figure 6) were 279°C and 179°C, and 141°C and 187°C for the ones applied on the lateral rubber surface (Points 2 and 1 in Figure 6). Instead, the temperatures in Isolators B and C were much lower and, except for the points in the bottom rubber layer, close to the bottom plate, (Points 12 and 19), never exceeded 100°C. Thus, it confirms that in order to meet fire resistance requirements, temperatures of the tested natural rubber

isolator should be maintained within the 100°C threshold. Moreover, since comparable temperatures were found for test B and C and the R90 requirement was met in both cases, 4 layers of insulation can be deemed sufficient for an effective fire protection.

The post-fire tests showed that, though the insulated seismic bearings were not significantly damaged, the loss of vertical stiffness is not fully recoverable after cooling. Indeed, the vertical secant stiffness K_v was reduced of 37.5% and 29.2% in the Isolators B and C respectively. The reduction of the vertical stiffness can be attributed to the marked and essentially irreversible thermal degradation of rubber. Conversely, no significant loss in vertical load-bearing capacity after the fire exposure was observed.

Table 7. Summary of the main results of the fire tests

Test	Failure time [min]	Temperature increase at failure [°C]		Maximum axial displacement [mm]	Vertical stiffness reduction after 92 min
		Minimum	Maximum		
A	61	85	279	4.08	//
B	> 92	31	242	5.55	37.5%
C	> 92	33	238	3.78	29.2%

4. Conclusions

In this work, the results of an experimental campaign carried out on seismic elastomeric bearings subjected to fire exposure are presented. Three natural rubber bearings were tested under the ISO 834 heating curve and by applying a constant vertical load equal to 900 kN. Two seismic isolators were protected with 100 mm, Test B, and 125 mm, Test C, of insulation blankets based on alkaline earth silicate wools (AES), whereas a third isolator, Test A, was not fire-protected. The tested seismic devices are part of an actual design project in Rome, in which the vertical elements should withstand the load-bearing capacity under the ISO 834 heating curve for 90 minutes. The experimental tests showed that only the protected rubber bearings met the fire requirement of 90 minutes. Indeed, the Isolators B and C did not fail for the entire duration of the fire test (92 min), while in Test A the unprotected isolator was not able to carry the applied load after 61 minutes. It can be concluded that

fire protection is necessary and that, for the insulation blanket employed in the tests, 100 mm of insulation are sufficient to provide an adequate fire protection.

More in detail, further considerations can be taken from the outcomes of the experimental campaign. First, temperature readings from the installed thermocouples indicated that when rubber layers exceeded a temperature value of about 180°C, rubber started suffering of a rapid deterioration of the mechanical properties that led to a progressive loss of the load-bearing capacity. This hints that a 150°C value represents a reasonable design threshold temperature, as can be found in literature. Moreover, except for the thermocouples close to the bottom plates of the isolators, in the protected seismic bearings the temperatures never exceeded 100°C throughout the entire fire test. This suggests to limit the temperature of such types of bearing below 100°C.

In general, temperatures measured inside the rubber bearing in the proximity of the steel plates were always higher than the others, proving that these regions are quite vulnerable to thermal attack owing to the heat sink effect of the steel plates. This aspect was particularly evident at the bottom plate, which was in contact with the terminal steel plate of the unprotected concrete-filled steel column. In this respect, the bottom plate of Isolators B and C detached after the fire test due to the excessive heating and the rubber in the proximity was deteriorated even though these isolators were protected. Thus, particular attention should be given to seismic bearings installed on the top of unprotected steel or steel-concrete composite columns and if vertical displacement has to be limited to avoid excessive differential displacements of the structure, adequate protection of the boundary conditions are required. Indeed, in these cases the heat transfer analysis in both the radial and in the vertical direction should be considered.

Finally, after the fire exposure the protected rubber bearings exhibited loss of about 1/3 of the vertical secant stiffness. In detail, the vertical secant stiffness K_v was reduced by 37.5% and 29.2% in Isolators B and C, respectively, and it can be attributed to the irreversible thermal degradation of rubber. Although no appreciable loss in vertical load-bearing capacity was observed, based on the stiffness reduction, substitution of the bearings is recommended.

Future perspectives will include numerical modelling of the test and comparison with design methods proposed in literature, as the isotherm method.

Acknowledgements

Nicola Tondini and Luca Possidente would like to acknowledge the support received from the Italian Ministry of Education, University and Research (MIUR) in the frame of the 'Departments of Excellence' (grant L 232/2016).

References

1. Kelly JM, Earthquake-resistant design with rubber, Springer-Verlag, London, 1997.
2. Peng Y, Huang T, Chen J, Experimental study of seismic isolated structures with sliding implant-magnetic bearings, Journal of Earthquake Engineering, 1-32, 2020.
3. Zheng W, Wang H, Li J, Shen H, Parametric study of superelastic-sliding LRB system for seismic response control of continuous Bridges, Journal of Bridge Engineering, 25(9), 2020.
4. Zheng W, Wang H, Li J, Shen H, Parametric study of SMA-based friction pendulum system for response control of bridges under near-fault ground motions, Journal of Earthquake Engineering, 25(8), 1494-1512, 2021.
5. Kelly JM, Konstantinidis D, Mechanics of rubber bearings for seismic and vibration isolation, Wiley, 2011.
6. Yoshida J, Abe M, Fujino Y, Constitutive model of high-damping rubber materials, Journal of Engineering Mechanics, Volume 130, Issue 2, 129 – 141, 2004.
7. Yamamoto S, Kikuchi M, Ueda M, Aiken I.D, A mechanical model for elastomeric seismic isolation bearings including the influence of axial load, Earthquake Engineering and Structural Dynamics, 38(2):157 – 180, 2009.
8. Kelly, J.M., Konstantinidis, D., Steel shim stresses in multilayer bearings under compression and bending, Journal of Mechanics of Materials and Structures, 4(6), 1109-1125, 2009.
9. Schleich JB et al., Development of design rules for steel structures subjected to natural fires in closed car parks, Technical Steel Research, ECSC, Report EUR 18867, Brussels, 1999.

10. Annerel E, Taerwe L, Merci B, Jansen D, Bamonte P, Felicetti R, Thermo-mechanical analysis of an underground car park structure exposed to fire, Fire Safety Journal, 57:96-106, 2013.
11. Nigro E, Cefarelli G, Ferraro A, Manfredi G, Cosenza E, Fire safety engineering for open and closed car parks: C.A.S.E. Project for L'Aquila, Applied Mechanics and Materials, 82:746-751, 2011.
12. Sommavilla M., Tondini N., Fire performance of a steel open car park in the light of the recent development of the localised fire model "LOCAFI", SiF 2020 - 11th International Conference on Structures in Fire, Brisbane, Australia, 30 November – 2 December, 2020.
13. Tondini N., Morbioli A., Vassart O., Lechêne S., Franssen J.-M., An integrated modelling strategy between FDS and SAFIR: Methodology and application, Journal of Structural Fire Engineering, 7 (3), 217-233, 2016
14. Possidente L., Weiss A., de Silva D., Pustorino S., Nigro E., Tondini N., Fire Safety Engineering principles applied to a multi-storey steel building, Structures and Buildings, 2020. DOI: 10.1680/jstbu.20.00110.
15. Derham CF, Plunkett AP, Fire resistance of steel laminated natural rubber bearings, NR Tech., 7(2), 29–37, 1976.
16. Liu WG, Zhou FL, Sun F, Huo D, Yan, WM, Product specification and mechanical properties of Chinese rubber bearings, Trans., 16th Int. Conf. on Structural Mechanics in Reactor Technology, International Association for Structural Mechanics in Reactor Technology, Raleigh, NC, 2001.
17. Kato A, Oba M, Michikoshi S, Minami T, Study on structural design for seismic isolated FBR: Part 28. Fire test results of rubber bearings, Summaries of technical papers of Annual Meeting Architectural Institute of Japan. B-2, Structures II, structural dynamics nuclear power plants, Architectural Institute of Japan, Tokyo, 1215–1216, 1999 (in Japanese).
18. Deckers X, Haga S, Sette B, Merci B, Smoke control in case of fire in a large car park: Full-scale experiments, Fire Safety Journal, 57:11-21, 2013.
19. Horvàth I, van Beeck J, Merci B, Full-scale and reduced-scale tests on smoke movement in case of car park fire, Fire Safety Journal, 57:35-43, 2013.

20. Bhowmick AK, Mukhopadhyah R, De SK. High temperature vulcanization of elastomers, Rubber Chem Technol 1979;52(4):725–34.

21. Kalpakidis IV, Constantinou MC, Effects of Heating on the Behavior of Lead-Rubber Bearings. I: Theory, Journal of Structural Engineering, 135(12): 1440-1449, 2009.

22. Kalpakidis IV, Constantinou MC, Effects of heating on the behavior of Lead-Rubber Bearings. II: Verification of Theory, Journal of Structural Engineering, 135(12): 1450-1461, 2009.

23. Wang H, Zheng W.-Z, Li J, Gao YQ, Effects of temperature and lead core heating on response of seismically isolated bridges under near-fault excitations, Advances in Structural Engineering, 22(14):2966 – 2981, 2019.

24. Mazza F, Nonlinear incremental analysis of fire-damaged R.C. base-isolated structures subjected to near-fault ground motions, Soil Dynamics and Earthquake Engineering, 77:192-202, 2015.

25. Mazza F, Residual seismic load capacity of fire-damaged rubber bearings of R.C. base-isolated buildings, Engineering Failure Analysis, 79:951-970, 2017.

26. Mazza F, Torsional response of fire-damaged base isolated buildings with elastomeric bearings subjected to near-fault earthquakes, Bulletin of Earthquake Engineering, 15(9):3673-3694, 2017.

27. Mazza F, Behaviour during seismic aftershocks of R.C. base-isolated framed structure with fire-induced damage, Engineering Structures, 140:458–472, 2017.

28. Mazza F, Alesina F, Fragility analysis of R.C. seismically-isolated structures with residual mechanical properties after fire exposure, Soil Dynamics and Earthquake Engineering, 121:383–398, 2019.

29. Wu B, Han L, Zhou F, Shen C, Tan P, Experimental Study on Fire Resistance of Building Seismic Rubber Bearings, Journal of Structural Engineering, 137(12):1593-1602, 2011.

30. Lan W, Qingsong G, Junsheng W, Jiangning W, Hongbo L, Research on Fire Resistance and Fire Protection of Seismic Rubber Bearings for Buildings, Journal of Tianjin University (Science and Technology), 53(11), 2020.

31. Wang L, Guan Q, Wang G, Pan Y, Zhan W, Liu H, Fire Test and Numerical Analysis of Large Size Seismic Rubber Bearings with Fire Protection Used in Beijing New International Airport, Journal of Tianjin University Science and Technology, Volume 51, Pages 119 – 126, 2018.

32. Decreto Ministeriale 1 febbraio 1986, Norme di sicurezza antincendi per la costruzione e l'esercizio di autorimesse e simili, Ministero dell'interno, Roma.
33. Decreto Ministeriale 14 gennaio 2008, Norme tecniche per le costruzioni, 2008, Ministero delle infrastrutture e dei trasporti, Roma.
34. European Committee for Standardisation (2004). Eurocode 2, Design of concrete structures - Part 1-2: General rules - Structural fire design
35. European Committee for Standardisation (2005), EN 1337-3:2005, Structural bearings - Part 3: Elastomeric bearings